Alexandria Engineering Journal (2022) 61, 10139–10152

HOSTED BY

Alexandria University

Alexandria Engineering Journal

www.elsevier.com/locate/aej
www.sciencedirect.com

Dual-layer hollow fibre haemodialysis membrane for effective uremic toxins removal with minimal blood-bacteria contamination

Sumarni Mansur [a], Mohd Hafiz Dzarfan Othman [a,*], Muhammad Nidzhom Zainol Abidin [b], Nik Ahmad Nizam Nik Malek [c], Ahmad Fauzi Ismail [a], Siti Hamimah Sheikh Abdul Kadir [d], Pei Sean Goh [a], Mohd Sohaimi Abdullah [a], Muhammad Hariz Asraf [c]

[a] *Advanced Membrane Technology Research Centre (AMTEC), School of Chemical and Energy Engineering, Faculty of Engineering, Universiti Teknologi Malaysia (UTM), 81310 Skudai, Johor, Malaysia*
[b] *Department of Chemistry, Faculty of Science, Universiti Malaya, Jalan Profesor Diraja Ungku Aziz, 50603 Kuala Lumpur, Malaysia*
[c] *Department of Biosciences, Faculty of Science, Universiti Teknologi Malaysia, 81310 Skudai, Johor, Malaysia*
[d] *Institute of Pathology, Laboratory and Forensics (I-PPerForM), Faculty of Medicine, Universiti Teknologi Mara (UiTM), Cawangan Selangor, 47000 Sungai Buloh, Selangor, Malaysia*

Received 13 January 2022; revised 27 February 2022; accepted 18 March 2022
Available online 31 March 2022

KEYWORDS

Dual-layer hollow fibre membrane;
Haemodialysis;
Antibacterial;
Urea and creatinine clearance

Abstract Bacterial endotoxin contamination in dialysate may pass through haemodialysis membrane and cause a silent chronic microinflammation to kidney patients. Dual-layer hollow fibre (DLHF) membranes with dual function, biocompatible adsorptive and antibacterial effects were developed to solve the problem of incompatible membrane and endotoxin contamination. All membranes were fabricated via the co-extrusion dry-wet phase inversion technique. In this study, silica/α-mangostin nanoparticle was incorporated into the inner layer of membrane to enhance the biocompatibility of the membrane while maintaining its adsorption capacity. Activated carbon (AC) was incorporated in the outer layer of membrane for improved antibacterial property. The DLHF membranes were characterised based on its morphology and surface hydrophilicity. The performance of the DLHF membranes was evaluated in terms of permeability, urea, and creatinine removal capabilities, bovine serum albumin (BSA) rejection and antibacterial properties. The dense and small pore size on the outer layer of AC created a smoother surface for the DLHF membrane. The BSA rejection of the DLHF membranes was enhanced by 6–8% compared to that of unmodified single layer hollow fibre membrane. Silica/α-mangostin nanoparticle in the inner layer of membrane enhanced the removal of urea and creatinine by chemisorption. Result also showed that the

* Corresponding author.
E-mail address: hafiz@petroleum.utm.my (M.H.D. Othman).
Peer review under responsibility of Faculty of Engineering, Alexandria University.

https://doi.org/10.1016/j.aej.2022.03.043

incorporation of AC in the outer layer of DLHF membrane successfully filtered bacteria by bacteria entrapment. DLHF membrane with the combination of silica/α-mangostin nanoparticle in the inner layer and AC in the outer layer possessed the higher bacteria inhibition into blood compartment against *Escherichia coli* and *Staphylococcus aureus*, with removal rate of 68% and 75%, respectively, and better urea and creatinine removal by 60.57% and 75.18%, respectively, compared to single-layer PSf based membrane. The development of co-adsorptive biocompatible DLHF membrane can play an important role in improvement of kidney patient life.

1. Introduction

Haemodialysis patients are exposed to approximately 300 – 600 L of water in a week, on average [1]. The high exposure of water leads to the possibility of contamination to waterborne pathogens [2]. Growth and lysis of these pathogens induce the pyrogenic fragments of bacteria such as endotoxins which is the fragment of bacterial cell wall that could lead to severe inflammation and multiorgan failure [3]. Bacterial pyrogen in dialysis fluid or dialysate may pass through the semipermeable membrane of haemodialyser and transfer into patients' blood [4]. The interaction of endotoxin and blood may potently initiate the activation of pro-inflammatory cytokines from monocyte that could induce acute and chronic side effect to haemodialysis patients [5–7]. To ensure the safety of the dialysate used during haemodialysis treatment, the Association for the Advancement of Medical Instrumentation (AAMI) and International Organization for Standardization (ISO) published the ISO 23500-5:2019 which states that the minimum quality requirements for dialysate used in haemodialysis treatment is less than 100 colony forming units (CFU)/mL and less than 0.5 endotoxin units (EU)/mL for bacteria and endotoxin, respectively [4].

The advancement in the development of haemodialysis membrane has provided better removal of uremic toxins for haemodialysis patients. Modifications on cellulose based membrane and polymeric based membrane have been progressively studied to achieve better quality of haemodialysis membrane [8–10]. The manipulation of the pore size and permeability of the membrane produces high flux hemodialyzer that can remove widest range of uremic toxins by allowing high fluid flow and convective transport [11–13]. Urea normal level in the blood for a healthy person, in general is approximately around 7–20 mg/dL [14]. Meanwhile, the normal range for creatinine in the blood is approximately around 0.84–1.21 mg/dL. In addition, accumulation of p-cresol in haemodialysis patient blood was closely related to the development of cardiovascular disease among the patients [15–17]. Elevated concentration of these uremic toxins indicated impaired kidney function [18,19]. At the same time, there are proteins that need to be retained during haemodialysis with molecular weight ranging from 64 to 66 kDa [20–22]. Clearance of these uremic toxins and retention of protein through semi-permeable haemodialysis membrane need to be achieved. However, there are concern in the use of high flux hemodialyzer as water pathogens can enter from the dialysate into the blood by back filtration (convective transfer) and back diffusion (movement down the concentration gradient) [11]. A study done by Henrie et al. [23] stated that there is presence of endotoxin in the blood circuit sample of mostly available haemodialysis membrane in the market except for thick-wall membranes.

In recent years, some strategies to retain and remove endotoxin from the dialysate have been studied by using sorbent or adsorptive membrane [24–26]. Dialysate passed through these adsorptive filters before entering the hemodialyzer. Based on the study done by Geremia et al. [26], activated carbon (AC) showed high percentage of bactericidal against *Escherichia coli* (*E. coli*) which are around 43%. However, direct contact of AC with blood may induce bio-incompatibility of the membrane [27]. The main purpose of incorporation of activated carbon into membrane is to avoid direct contact of the activated carbon with blood. Haemodialysis application required unfiltered blood to be filtered outside of human body by haemodialyser. Thus, it is important to ensure the biocompatibility of the material that will be in contact with the blood as the filtered blood will enter back into human body. Any incompatibility will cause side effect to the patient. The complications arisen from the direct contact of blood and AC and the indiscriminate adsorption of life sustaining molecules including plasma proteins present in human blood become the concerns. Therefore, dual-layer hollow fibre (DLHF) membrane which consist of AC in the membrane outer layer was developed to prevent direct contact of AC with blood [27,28]. The membrane will be thick and high concentration of AC with antibacterial properties would be concentrated in the outer layer of the membrane to inhibit the bacteria or endotoxin transfer as shown in Fig. 1. Most of these studies focus only on using adsorbent on either inner or outer layer of the DLHF membrane as shown in Table 1. By incorporation of adsorbent in either side of the membrane, the direct contact of bio-incompatible adsorbent can be avoided. However, the adsorption of the adsorbent and adsorbate occurs at the blood/membrane interface. Thus, the incorporation of adsorbent in outer layer of the DLHF membrane would not be strong enough to adsorb the uremic toxins in blood compartment.

The main objective of this study is to fabricate a biocompatible, adsorptive and antibacterial PSf based DLHF membrane embedded with inorganic particles via a single-step coextrusion technique for haemodialysis application. To achieve both biocompatible membrane with better clearance of uremic toxins and prevention of bacterial penetration into blood compartment, DLHF membranes with two types of adsorbents in inner and outer layer composition were developed. Novel biocompatible composite nanoparticle from our previous work, silica/α-mangostin nanoparticle was incorporated into the inner layer of the membrane to improve the biocompatibility of the membrane when in contact with blood while maintain-

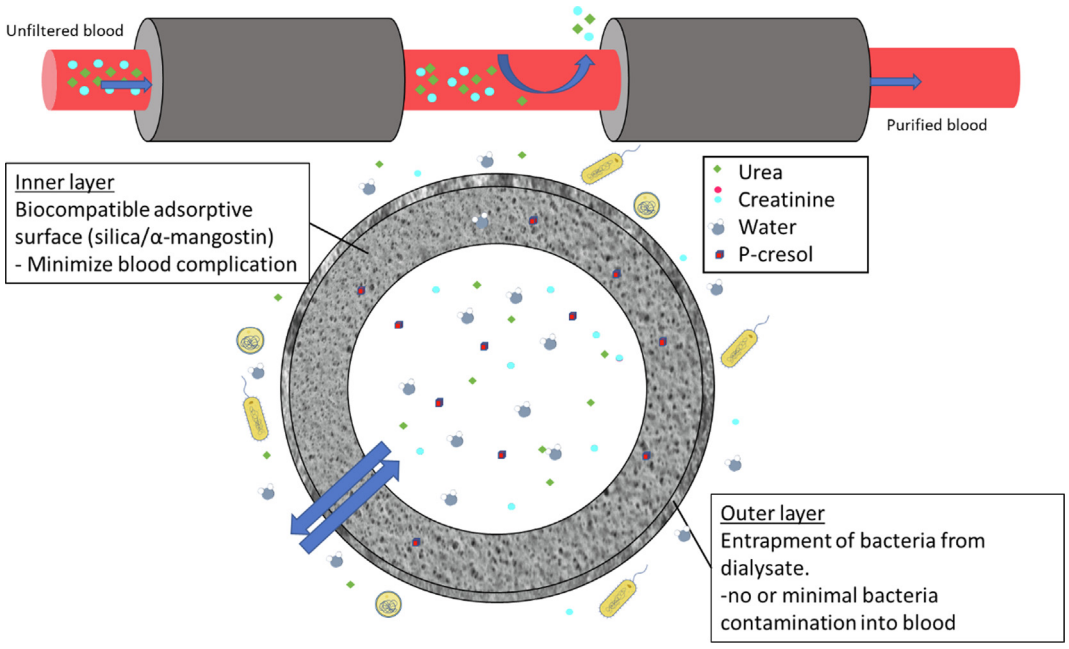

Fig. 1 The mechanism of DLHF membrane in uremic toxins removal and entrapment of bacteria.

Table 1 Studies on DLHF membrane for haemodialysis application.

Membrane	Inner layer	Outer Layer	Spinning technique	Dual-function	Main toxins removal	Reference
Dual-layer MMM	PES/ PVP	PES/PVP/AC	Casting	combining diffusion and adsorption in one step	Creatinine, Para-aminohippuric acid	[28]
PES/AC	PES/ PVP	PES/PVP/AC	Dry-wet spinning	Avoid blood-sorbent contact	Creatinine, p-cresylsulfate	[37]
MMM double layer	PES/ PVP	PES/ PVP/modified AC	Casting	Avoid blood-sorbent contact	Creatinine	[39]
PSf/N-PMMA	PSf/ PVP	PSf/N-PMMA/PVP	Dry-wet spinning	combining diffusion and adsorption in one step	Urea, Creatinine	[31]
Low-flux MMM	PES/ PVP	PES/PVP/AC	Dry-wet spinning	Avoid contact with AC Good haemocompatibility	Albumin	[36]
Dual-layer MMM	PES/ PVP	PES/PVP/AC	Dry-wet spinning	complete removal of endotoxins from dialysate and preventing transfer of endotoxins to the blood compartment while at the same time achieving high removal of uremic toxins from human plasma	Lipopolysaccharades from E.coli, Indoxyl sulphate, hippuric acid	[26]
MMM-OIF	PES/ PVP/ AC	PES/PVP	Dry-wet spinning	Outside-in-filtration, Prevent fiber clotting Combine diffusion and adsorption	Urea, creatinine, indoxyl sulphate, hippuric acid	[40]

ing its adsorption capacity [29]. Simultaneously, AC was incorporated in the outer layer of the membranes to prevent the bacteria contamination in blood compartment. Based on our previous work, the maximum adsorption capacity for the composite nanoparticle for p-cresol is 55.64 mg/g at 500 mg/L p-cresol initial concentration and improved the antioxidant properties of the membrane [29]. The incorporation of the composite nanoparticle in the inner layer of the membrane can improve the biocompatibility of the membrane when in contact with blood, hence minimizing the biocompatibility issues of haemodialysis membrane. To avoid delamination of DLHF membrane, PSf polymer was used as the main polymer for both inner and outer layer of the membrane. The morphological structure, performances of the membrane to remove urea and creatinine, and the bacteria filtration capability of the membrane were evaluated and compared to single layer hollow fibre membrane.

The rationale of this research is to explore the development of biocompatible and adsorptive membranes for haemodialysis application. This study would have brought upon a huge importance towards multiple fields of research which includes nanotechnology, membrane technology and nephrology. The

primary outcome of the research would benefit the scientific community in the sense of filling in the knowledge gap in those fields.

2. Experimental

2.1. Materials

69,500 g/mol of polysulfone (PSf, udel-1700) was chosen as the base membrane. This polymer was obtained from Solvay Advanced Polymers. N-methyl-2-pyrrolidine (NMP) which acts as the solvent, was purchased from Sigma-aldrich, USA. 360,000 g/mol hydrophilic additive polyvinylpyrrolidone (PVP) was obtained from Sigma-aldrich. Coconut shell AC and silica nanoparticle were purchased from Sigma-aldrich, USA. Bovine serum albumin (BSA), p-cresol, urea, creatinine, homocysteine, and lysozyme were obtained for Sigma-aldrich, USA. ATC 11,229 and ATCC 6538 of gram-negative *E. coli* strain and gram-positive *S. aureus* strain, respectively were cultured in petri dish and used throughout the study. Composite nanoparticle nanoparticle was synthesised using the same sol–gel nanofabrication technique as in our previous study [29]. Alpha-mangostin (BOC Sciences, USA) was mixed into silica solution. The solution was left to gel for 48 h and incubated in the oven at 50 ℃ and grinded to nanosized. The composite nanoparticle was labelled as silica/α-mangostin nanoparticle.

2.2. Dope solution preparation

PSf, PVP, AC and silica/α-mangostin nanoparticle were dried at 50℃ overnight prior to the preparation of the dope solutions. The dope solution composition for each membrane was shown as in Table. 2. Neat SLHF membrane without any addition of outer dope solution was labelled as M0. M01 and M02 composed of same composition of outer dope solution but different composition of inner dope solution. The composite nanoparticle or AC was first dissolved in NMP solvent and stirred using overhead mechanical stirrer continuously for one hour or until all the nanoparticle was completely dissolved and homogenous in the solvent. Next, PVP was poured into solution containing the nanoparticle and stirred continuously for another 2 h. Lastly, PSf was added and stirred overnight until all the polymers completely dissolved.

2.3. Hollow fibre membrane fabrication

The DLHF membranes were spun using co-extrusion spinning technique as described by Dzinun et al. and Abidin et al. [30,31]. The spinneret was connected to two gear pumps, one gear pump was connected to inner dope reservoir, while another one gear pump was connected to the outer dope reservoir, as illustrated in Fig. 2. Inner dope solution was extruded out from the spinneret at 8 mL/min, followed by the bore liquid with the same flow rate, 8 mL/min. Once the inner layer of the membrane was forming, 1 mL/min of the outer dope solution was released from the spinneret. Table 3 shows the spinning conditions for the fabrication of the DLHF membrane. The fabricated DLHF membranes were soaked in running tap water for 48 h to remove all the residual NMP solved in the membrane. The membranes were then treated with 10% glycerol where the membranes were immersed for 24 h to prevent the structure of the membrane from collapsing. Prior to storage, the DLHF membranes were air-dried at room condition.

2.4. Characterisation of fabricated DLHF membranes

The DLHF membranes were characterised based on scanning electron microscopic (SEM) images, energy dispersive X-ray (EDX) analysis, atomic force microscopic (AFM) images and inner surface contact angle goniometer. The cross-sectional and surface morphology of the DLHF membranes were characterised using the scanning electron microscope (SEM, Hitachi, USA). The cross-sectional surface of the membrane was prepared by a freeze fracturing technique. Snapping of the membrane in liquid nitrogen helped in obtaining a smooth cutting of cross-sectional surface. The surface of the membrane was prepared by cutting 1 cm length of the membrane. The prepared samples were placed on stab. Prior to the SEM analysis, the sample was sputter-coated with gold to avoid noise ratio. EDX was used to determine and quantify the elemental composition of the hollow fibre membrane. At 15 kV accelerating voltage, the sample was evaluated. At a magnification of 250×, each sample's mapping and spectral point images were examined and analysed. Carbon (C), oxygen (O), sulphur (S), and silicon (Si) atomic concentration were all determined. To get an average value, the analysis was performed three times. The surface roughness of the membrane was determined by SE-100 atomic force microscope (AFM, Park System). 2 cm of the membrane samples was cut and scanned by tapping mode with the scanning area of 10 μm × 10 μm. Contact angle goniometer (Dataphysics, Germany) was used to analyse the inner surface hydrophilicity property of the membranes. 0.2 μL water was dropped on the surface of the membrane at fixed 1.0 μL/s of dosing rate using the sessile drop method. The shadow of the water droplet on the membrane was captured and recorded. The contact

Table 2 Neat SLHF and DLHF membrane dope composition for inner and outer layer of the membrane.

Membrane	Inner dope (wt%)				Outer dope (wt%)			
	PSf	PVP	NMP	Silica/α-mangostin	PSf	PVP	NMP	AC
M0	18	3	79	–	–	–	–	–
M01	18	3	79	–	15	5	78	2
M02	18	3	77	2	15	5	78	2

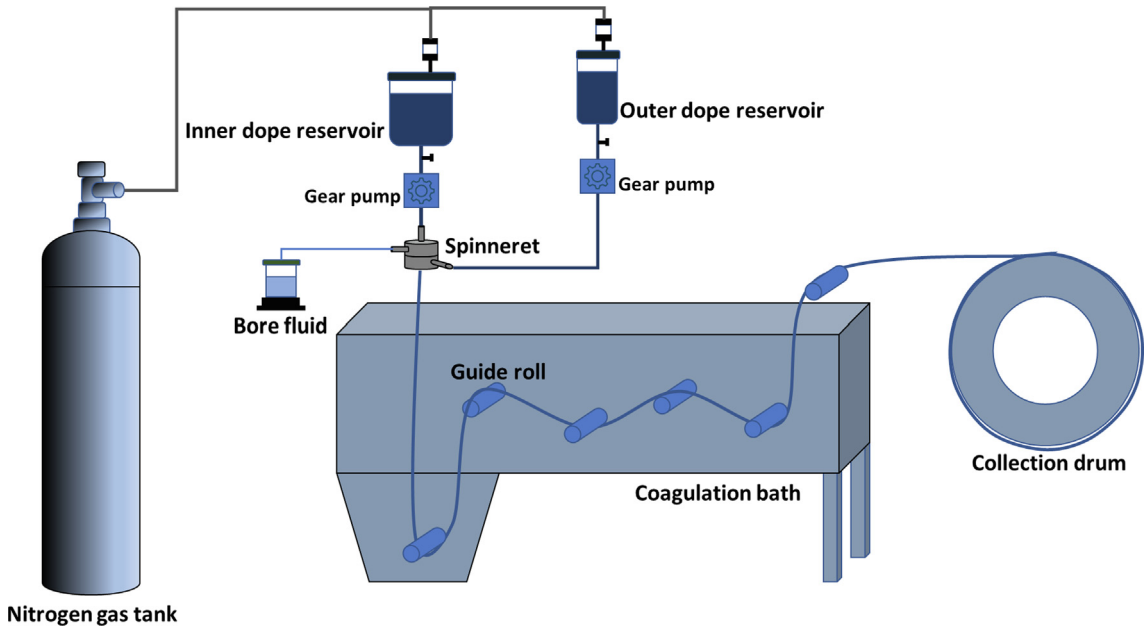

Fig. 2 Schematic diagram of co-extrusion phase inversion spinning technique for DLHF membrane.

Table 3 Spinning conditions for DLHF membranes fabrication.

Spinning Condition	
Spinneret/water surface distance (cm)	30
Inner dope extrusion rate, DER (ml/min)	8
Outer DER (ml/min)	1
Bore liquid	Reverse osmosis water
Coagulation bath	Tap water
Bore liquid flow rate, BLFR (ml/min)	8
Pulling wheel speed (rpm)	4
Coagulation bath temperature	Room temperature

angle for each fibre was measured 10 times to get a reliable measurement.

2.5. Membrane performance analysis

2.5.1. Membrane flux and permeability

The permeability of the fabricated membrane was determined using tap water at a fixed pressure of 0.5 bar. The flux and permeability of the membrane was tested through a crossflow ultrafiltration experiment system. Prior to the testing, the feed (tap water) was allowed to pass through the lumen of the membrane for 40 min at 1.0 bar to ensure water filled up the membrane and pressure are stabilised. Next, the permeation of the water was collected and measured for every 10 min. The testing was repeated 3 times to obtain an average value. The permeability of the membrane was calculated from the Eq. (1).

$$\text{Permeability}(\text{L/m2} \cdot \text{h} \cdot \text{bar}) = \frac{V}{A \times \Delta t \times P} \quad (1)$$

where V indicated the volume of permeate (L) over the area of the hollow fibres, A (m^2), the time taken, t (h), and the pressure, P (bar).

2.5.2. Dialysis

The hollow fibre membranes were subjected to 4 h of dialysis using the crossflow ultrafiltration experiment system. Water in the beaker acts as dialysate where the waste substances from the blood enter the membrane. A solution with the mixture of red blood cell, 0.9% saline solution, 1500 ppm urea, 1000 ppm creatinine, and 500 ppm bovine serum albumin (BSA) was prepared. The permeate was taken for each hour of the dialysis process. The solute concentration in each sample was analysed using urea assay kit, BSA assay kit and creatinine assay kit. All the kits were obtained from BioAssay System, USA. The samples were prepared as described in the kit's manual description. The prepared samples were read at 520 nm using microplate spectrophotometer (Thermo Scientific, Finland). The test for each sample was replicated 3 times for every sample to obtain an average value. High performance liquid chromatography (HPLC) from Agilent, USA was used to determine the p-cresol concentration. All samples were tested using C18 stationary column (5 μm Zorbax) of 4.6 × 250mm (Agilent, USA) at 254 nm wavelength. 40:60 ratio of ultrapure and acetonitrile was used throughout the testing process (0.5 mL/min flowrate, 7 min retention time). The dynamic adsorption-filtration of urea and creatinine was determined using formula in Eq. (2),

$$\text{C} = [C_i - C_f] \quad (2)$$

where C represents the uremic toxins concentration, while C_f is the final concentration and C_i is the feed initial concentration.

2.5.3. BSA rejection

67,000 g/mol of BSA served as the protein marker for the rejection test. Ultrafiltration experiment system was used to determine the BSA rejection. BSA solution (500 ppm) was run through the system and the permeate was collected. UV-spectrophotometer (DR-5000TM, Canada) was used to determine the concentration of BSA in the permeate. The test was retested for 3 times to obtain an average value. The percentage of rejection, R (%) was measured using Eq. (3),

$$R = [1 - \frac{C_p}{C_F}] \times 100\% \quad (3)$$

where R represents the percentage of BSA rejection, C_P is the concentration of the permeate solution and C_F is the concentration of the feed solution.

2.5.4. Sieving coefficient

Different types of uremic toxins solutes were used to investigate the ability of the membrane in sieving the small molecules (urea and creatinine), middle molecules (homocysteine), large molecules (lysozyme) and protein (BSA). 1500 ppm urea, 1000 ppm creatinine, 100 ppm homocysteine, 400 ppm lysozyme were dissolved in RO water. UV-spectrophotometer (DR-5000TM, Canada) was used to determine the concentration of uremic toxins in the permeate. The sieving coefficient (SC) of the solutes was calculated using Eq. (4) and repeated three times to get a reliable value.

$$SC = \frac{C_P}{C_f} \quad (4)$$

2.6. In-vitro filtration of dialysate contaminated with bacterial culture

E. coli (ATCC 11229) and *S. aureus* (ATCC 6538) bacteria were streaked on nutrient agar (NA) plate by streaking method to obtain a single colony. The NA plate containing bacteria was incubated at 37 ℃ overnight. About 5–10 colonies were selected using a sterile inoculating loop and inoculated in 20 mL of nutrient broth (NB) and incubated at 37 ℃ for 24 h. The solution was agitated at 200 rpm overnight and labelled as bacteria suspension solution. About 10 mL of the bacteria stock suspension was mixed with 90 mL of the Luria-Bertani (LB) broth, and the solution was transferred into 50 mL centrifuge tube. The solution was centrifuged at 4000 rpm for 15 min. The pellet was washed using sterilized distilled water for 3 times. The resultant pellet was suspended in 200 mL of sterilized distilled water. This solution containing the bacteria acted as dialysate during the ultrafiltration permeation test.

Prior to permeation testing, the membrane samples were sterilised under UV radiation for one hour and all the glassware was sterilised using an autoclave. The permeation of the dialysate containing bacteria was analysed using the cross-flow ultrafiltration system. The DLHF membranes were pressurised with 0.5 bar and the permeation was collected every one hour. Accurately, 100 μL of the permeate solution was mixed with 900 μL of distilled water to make a ten-fold dilution. A serial dilution was performed to determine the minimum inhibitory concentration (MIC) and minimum bacterial concentration (MBC) values. Accurately, 10 μL of each dilution was transferred on prepared Mueller-Hinton agar (MHA) plate. The MHA plate was placed in an incubator upside down and incubated at 37℃ overnight. The number of growth colonies was observed and calculated. The bacterial removal was calculated using Eq. (5).

$$Bacterial\ removal(\%) = \left[\frac{A - B}{A}\right] \times 100\% \quad (5)$$

where A represents the number of bacterial colonies on MHA agar plate of the solution containing bacteria prior to permeation test. B represents the number of bacterial colonies on MHA agar plate from permeate solution of tested membrane.

2.7. Membrane biocompatibility analysis

The ability of the DLHF membrane to inhibit or decrease the cells damage caused by hydrogen peroxide (H_2O_2) and nitric oxide (NO) can determine the antioxidant characteristic of the DLHF membrane. 50 mM of 30% of H_2O_2 was added into 20 mL of distilled water. The DLHF membrane was weight 0.5 g and the membrane was immersed in 1 mL of H_2O_2 solution. The solution containing the membrane was placed at 27 ℃ for 30 min. The concentration of H_2O_2 before and after reaction with the DLHF membrane was determined using DIOX-250 peroxide assay kit obtained from BioAssay, USA. The assay was read at wavelength 540 nm on microplate spectrophotometer. Percentage of H_2O_2 scavenging activity was calculated using Eq. (6).

$$\%scavenging\ activity = \frac{Control\ absorbance - sample\ absorbance}{control\ absorbance} \times 100 \quad (6)$$

20 mM of Sodium nitroprusside (SNP) was dissolved in phosphate buffer saline (PBS) solution. SNP was used to produces NO. Reaction between NO and oxygen produced nitrite ion. Next, 0.5 g of DLHF membrane was dipped in the solution. The solution containing the membrane was sit at room temperature for 20 min. Each solution of the sample was added with Griess reagent to quantify the concentration of nitrite ion produced. The assay was analysed at 546 nm. Addition of the membrane was expected to reduce the nitrite ion production. The percentage of NO scavenging activity was determined using Eq. (6).

The complement 5a (C5a) expression of the whole blood determined the coagulant activity of the blood after in contact with the membrane. C5a expression was measured using a C5a ELISA kit (Cusabio®, China). For 1 h, a DLHF membrane sample was submerged in PBS solution. The DLHF membrane was then added to 1 mL of whole blood and incubated at 37 °C for an additional 2 h. The blood containing the membrane sample was centrifuged at 1500*g* for 15 min to separate the whole blood. Platelet poor plasma (PPP) from centrifuged whole blood was pipetted into an ELISA kit assay and analysed with a microplate reader at 450 nm (Thermo Scientific, Finland). To obtain a reliable value, each sample was repeated three times.

3. Results and discussion

3.1. Membrane characteristics

The morphological property of the DLHF membranes was observed based on the SEM images, as shown in Fig. 3. Based on Fig. 3, the membrane formed a dense skin layer at innermost and outermost layer of the membrane. While a sponge-like layer was produced in the middle of the membrane [32]. The addition of PVP increases the viscosity of the membrane and helps in hindering the diffusional rate during the phase inversion of the membrane. Thus, producing the sponge-like layer with finger-like structure in the middle of the membrane that subsequently affect the flux of the membrane [33]. For DLHF membranes, the outer layer of the membrane was extruded out after the inner layer of the membrane has been stabilised to ensure the mixing of both dope solutions during the co-extrusion. PSf polymer was used as the base membrane for inner and outer dope solution to create a mutual diffusion during phase inversion process. Due to this the DLHF membranes show no sign of delamination between two layers and no apparent gaps appear. Delamination of membrane can be described as a defect membrane. Delamination occurs when the outer layer detaches from the inner layer. The outer and inner layer did not form a uniform structure. Thus, delamination can affect the performances of the membrane. A microporous sponge-like sub-layer beneath the outer skin layer as shown on Fig. 3(2b) and (3b) indicate the second layer of the DLHF membrane which was different from the outer structure of SLHF membrane in Fig. 3(1b). The changes in the membrane pore size at the sublayer can be obviously seen on their outer surfaces, as shown in Fig. 3(1c, 2c and 3c). The outer surface of M02 membrane which comprised of AC in the outer layer had a denser and more rigid structure of outer surface with smaller pore size.

Fig. 4 shows the EDX mapping conducted on the neat PSf SLHF membrane, M0, DLHF membrane containing AC, M01 and DLHF membrane containing silica/α-mangostin in inner layer and AC in outer layer, M02. All the membranes consisted of carbon, oxygen and sulphur, which represent the chemical structure of the main polymer, PSf. Based on Fig. 4, the yellow dots represent the silicon element. These yellow dots were only detected and clearly observed in M02 membrane, spread at the inner side of the membrane. This signifies the presence of silica nanoparticle in the inner layer of the membrane. However, no significant difference can be seen at the outermost side of M01 membrane (Fig. 3(b)), compared to M0 membrane (Fig. 3(a)), since there was no characteristic element present. AC is pure carbon and the most abundant element in PSf chemical structure is also carbon.

In haemodialysis application, rough membrane surface would promote the adhesion of platelets and create biofouling on the membrane surface [34,35]. Fig. 5 shows the 3D AFM images of membrane outer surface with different degrees of roughness. The neat PSf SLHF membrane, M0, displayed a

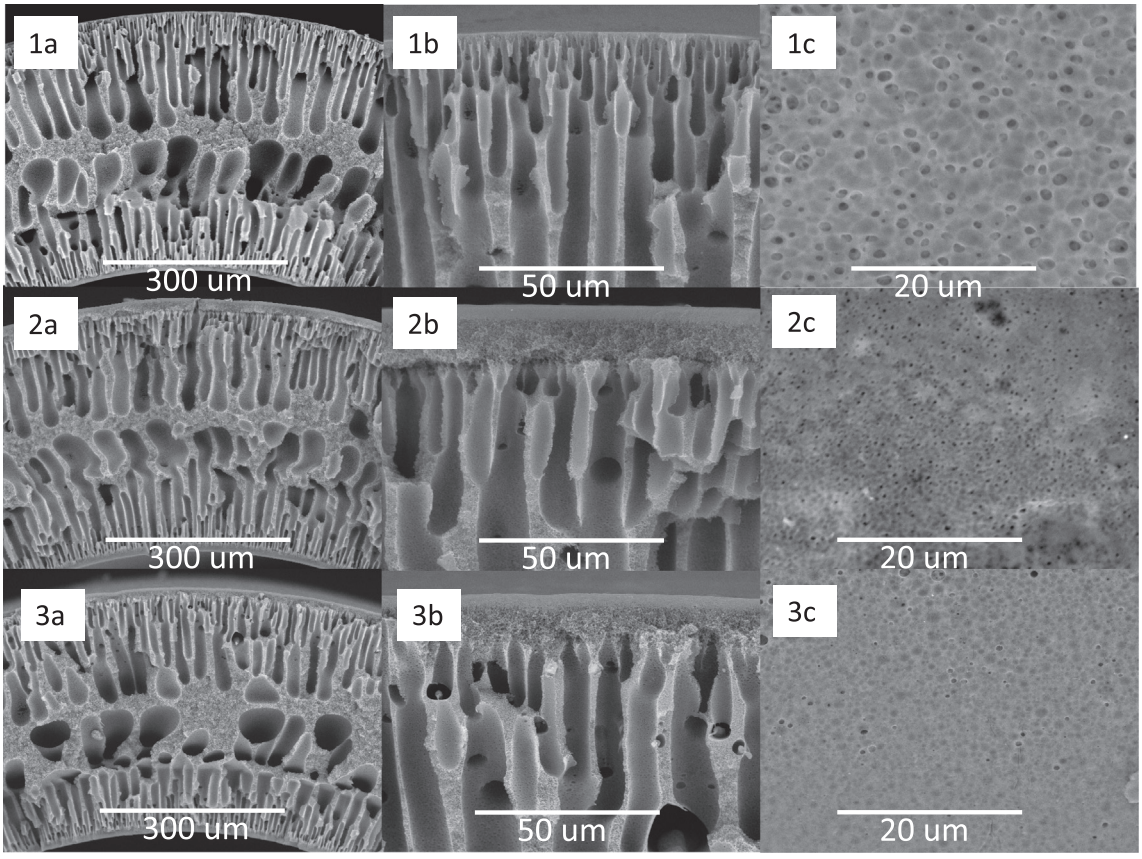

Fig. 3 SEM images of neat SLHF M0 (1) and DLHF membrane, M01 (2), and M02 (3). Cross-sectional area of the membrane (a) 1500× magnification. (b) 300× magnification. (c) Outer membrane surface at 5000× magnification.

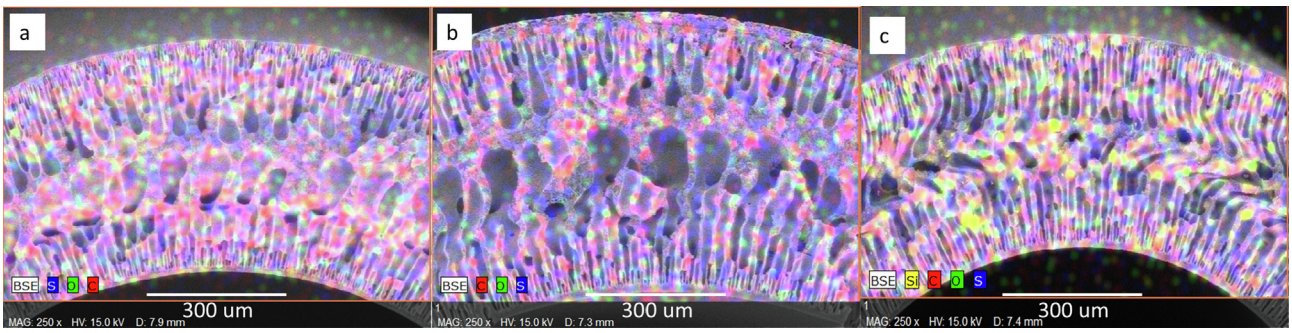

Fig. 4 EDX mapping of DLHF membrane M0 (a), M01 (b) and M02 (c) at 250× magnification.

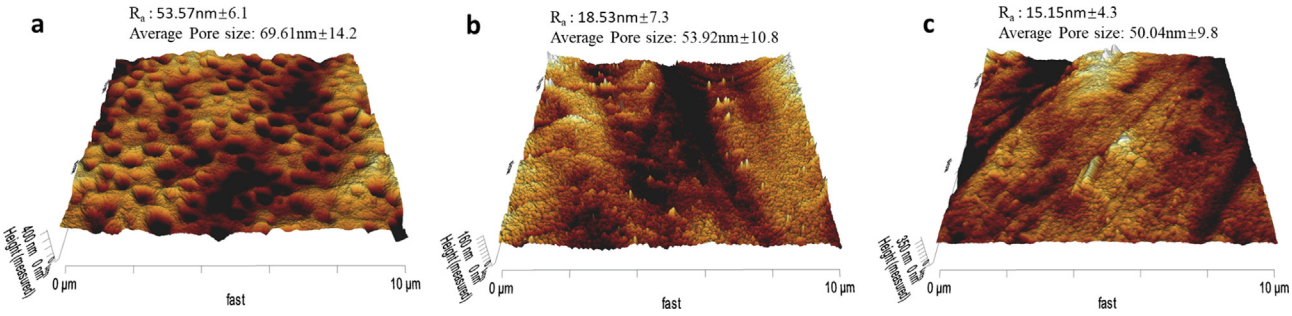

Fig. 5 AFM images of the surface of SLHF membrane M0 (a) and DLHF membrane M01 (b) and M02 (c), M02 (c). R_a indicates the average surface roughness of the membrane outer layer. 3 images were obtained for each membrane.

rough surface with an average surface roughness of 53.57 nm. On the contrary, the surface of M01 (Fig. 5(b)) and M02 (Fig. 5(c)) membranes, which contained AC in the membrane outer layer, was smoother with an average surface roughness of 18.53 and 15.15 nm, respectively. This was believed to happen due to the regular collocation of the AC in PSf matrix.

3.2. Membrane filtration performance

The water permeability and surface hydrophilicity of a membrane are related to the membrane morphological structure.

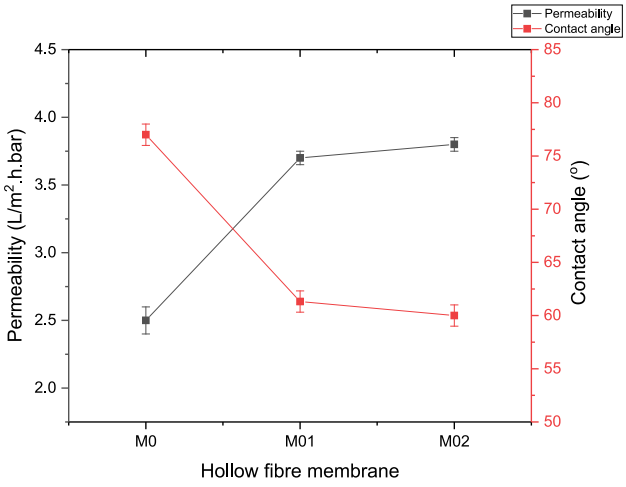

Fig. 6 Permeability and surface contact angle measurement of membrane M0, M01, and M02. Standard deviation is represented by the error bars ($n = 3$).

Fig. 6 depicts the link between water permeability and water contact angle in DLHF membranes. The water permeability of M0, M01, and M02 is 2.3, 3.7, and 3.8 L/m^2·h·bar, respectively. The interrelationship between water permeability and water contact angle of the DLHF membranes can be observed in Fig. 6. M02 membrane had the highest water permeability of 3.8 L/m^2·h·bar. The presence of AC in the membrane outer layer helped in improving the surface hydrophilicity of the membrane. As the result, the water permeability of the membrane increased by 54.5% compared to M0 membrane. The high-water uptake of the membrane was due to the bonding of water molecules with the oxygenated surface sites of AC (18). The incorporation of silica/α-mangostin in the inner layer of the DLHF membrane enhanced the surface hydrophilicity and the water permeability of the membrane M02. The presence of OH group in silica nanoparticle induced the membrane's interaction towards water molecules [35]. M02 membrane which composed of silica/α-mangostin in inner layer and AC in outer layers displayed lower water contact angle and higher water permeability than M01 membrane.

Prior to dialysis experiment, the water permeability of the membranes, using blood solution as feed, was recorded for 4 h of cross-flow filtration, as shown in Fig. 7(A). Throughout the filtration, there was no blood leaked out through the membrane into the permeate, as shown in Fig. 7(B). This was due to the large size of red blood cell that prevented it from passing through the membrane. Based on the result in Fig. 7(A), the water permeability of the neat PSf SLHF membrane, M0 showed the fastest dropping rate, started after 120 min of filtration. The rough surface of M0 membrane has caused the biofouling to occur faster compared to DLHF membranes.

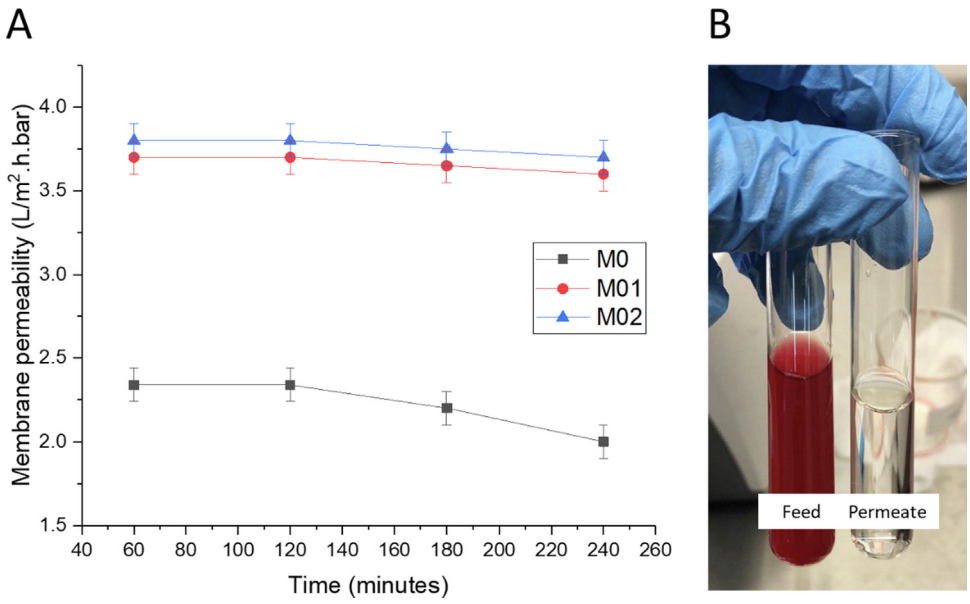

Fig. 7 (A) Permeability of fabricated membranes (M0, M01, and M02) over time. (B) The colour changes of solute containing red blood cell, urea, creatinine and BSA before and after dialysis. Standard deviation is represented by the error bars. The experiment was repeated 3 times to obtain reliable results. (For interpretation of the references to colour in this figure legend, the reader is referred to the web version of this article.)

Meanwhile, M01 and M02 membranes showed the same pattern of water permeability decline over 4 h of filtration.

The separation performance of DLHF membranes was further investigated based on 4 h of dialysis. Blood solution containing a mixture of red blood cell, 0.9% saline solution, 1500 ppm urea, 1000 ppm creatinine, 500 ppm p-cresol and 500 ppm BSA was used as feed. RO water was used as the dialysate. The membranes were evaluated based on their capability to remove small molecular uremic toxins which are urea and creatinine, and a protein bound uremic toxin which is p-cresol. Fig. 8 shows the percentage of urea and creatinine removal after 4 h of dialysis. It can be suggested that the removal of urea and creatinine was primarily based on diffusion with the help convection. The difference of solute concentration in feed and dialysate created a concentration gradient to the solutes. Both urea and creatinine diffused from the higher solute concentration region (blood solution) to the lower solute concentration region (dialysate) [34]. At the same time, the transmembrane pressure also pulled water from blood solution into dialysate which caused urea and creatinine to be removed along via convection.

The presence of silica/α-mangostin nanoparticle in the inner layer of M02 membrane enhanced the removal of urea and creatinine. M02 membrane obtained the highest percentage of urea and creatinine removal of 60.6% and 75.2%, respectively. The main difference of M01 and M02 is the present of silica/α-mangostin nanoparticle in the inner layer of the membrane. Mansur et al found that silica/α-mangostin nanoparticle possessed highly porous structure and contain functional OH groups [29]. These properties have contributed to the enhancement of the membrane water permeability by enhancing the capability of the membrane to capture more water, simultaneously improve the removal of uremic toxins through convection.

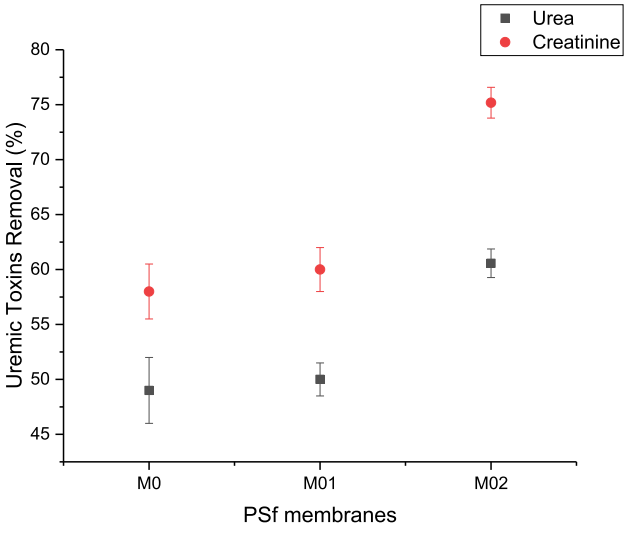

Fig. 8 Percentage of uremic toxins removal for 4 h on DLHF membranes (M0, M01, and M02) with urea and creatinine initial concentration of 1500 ppm and 1000 ppm, respectively. Standard deviation is represented by the error bars. The experiment was repeated 3 times to obtain reliable results.

Fig. 9 shows the change of p-cresol concentration in the feed during dialysis for a total of 4 h. P-cresol can be removed from the blood via diffusion into the dialysate and via adsorption onto the membrane surface. The decreased p-cresol concentration in the feed represents the total removal of p-cresol from blood, either by diffusion or adsorption. The concentration of feed solution containing p-cresol decreased as the duration of dialysis increased. The presence of composite

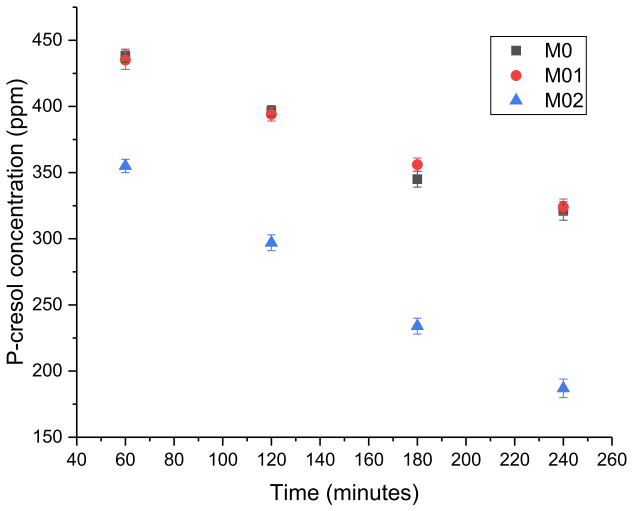

Fig. 9 DLHF membrane dynamic adsorption-filtration study (M0, M01, M02, D01 and D02). Standard deviation is represented by the error bars. The experiment was repeated 3 times to obtain reliable results.

nanoparticle in the inner layer of the membranes enhanced the removal of p-cresol by adsorption method. Moreover, the addition of silica nanoparticle and AC in the outer layer of the membrane did not affect the membrane separation performance as the separation process takes place mainly at the inner side of the membrane.

Fig. 10 shows the result of BSA rejection for all the fabricated membranes. All membranes maintained high BSA rejection, which was more than 80% throughout the 4 h of dialysis. High percentage of rejection means that the membranes can retain essential proteins in blood. Compared to the neat PSf SLHF membrane, M0, DLHF membranes containing AC in the outer layer, M01 and M02 showed higher BSA rejection

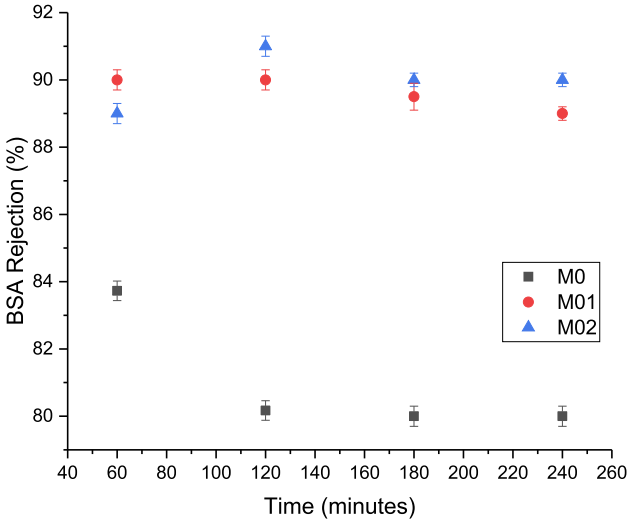

Fig. 10 BSA rejection of fabricated membranes (M0, M01, M02, D01 and D02) over time. Standard deviation is represented by the error bars ($n = 4$).

showed a better BSA rejection performance. M01 and M02 membranes rejected 90% and 89% of BSA, respectively, after the first hour of dialysis. Meanwhile, M0 membrane can only reject 83.7% of BSA after one hour of dialysis. These results were in agreement with the morphology of the produced membranes. DLHF membranes had a thicker wall and a smaller pore size as compared to SLHF membrane. Thus, DLHF membranes possessed a higher resistance against large proteins like BSA. However, after 120 min, both M01 and M02 shows a decrease in BSA rejection percentage. This fact may be due to the plugging of more BSA molecules on the membrane surface and inside the pores has created additional pressure. This has enhanced the convection to push the large BSA molecules, squeezing into the pores, moving pass the membrane wall.

However, study done by Geremia et al. showed protein rejection more than 90% for all membranes fabricated in their study [36]. The difference size of spinneret used in Geremia et al. study and in this study influenced the pore size produced, the higher pore size of the membrane in this study was one of the reasons that caused the lower protein rejection, thus explaining the differences in the protein rejection results.

Table 4 summarises the comparison between DLHF membranes fabricated in this study and the DLHF membranes previously developed by Pavlenko *et al.* (2016) and Abidin *et al.* (2019) for haemodialysis application. The membrane performance in terms of the water permeability and the urea and creatinine removal was compared. Based on the comparison, PSf DLHF membrane containing silica/α-mangostin in the inner layer and AC in the outer layer developed in this study clearly can be a strong membrane candidate for haemodialysis application due to the high removal of uremic toxins and the comparable water permeability. It is worth mentioning that the membrane was capable to effectively remove urea, creatinine and even p-cresol from the real blood sample.

3.3. Bacterial culture filtration and adsorption using DLHF membrane

E. coli (Gram-negative) and *S. aureus* (Gram-positive) have been selected as model bacteria to demonstrate the bacteria filtration of the fabricated membranes. Bacteria suspension of *E. coli* and *S. aureus* with initial bacterial concentration of 10^8 CFU/mL was used feed solution and filtered through the prepared DLHF membranes. The bacteria removal was determined by analysing the bacteria content in filtrate. Table 5 shows the bacteria removal of the membranes against *E. coli* and *S. aureus*. The neat PSf SLHF membrane, M0, had the ability to filter 50% of both bacteria. The ultrafiltration range of pore size of the M0 membrane has made the membrane possible to filter the bacteria with the size ranges from 0.5 to 5 μm in length [42,43]. Compared to M0 membrane, DLHF membranes with different combinations of inner and outer layer compositions possessed an increase in bacteria removal. AC has the capability to entrap the bacteria, thus preventing the bacteria from passing through the haemodialysis membrane. AC entraps the bacteria via adsorption mechanism using macropore, mesopore and micropore of the particles [43]. The porous structure of AC in M01 and M02 membranes captured the bacteria efficiently and adsorbed the bacteria on the pore surface of the particle.

Table 4 Comparison between different DLHF membranes for haemodialysis application.

	Inner layer	Outer layer	Spinning technique	Permeability (L/m^{2}h) at 0.5 bar	Urea removal (%)	Creatinine removal (%)	References
PSF/Si-mangostin DLHF	PSf/PVP/Si-mangostin	PSF/PVP/AC	Dry-wet spinning method	3.81	60.57	75.18	In this study
Double layer MMM	PES/PVP	PES/PVP/AC	Dry-wet spinning method	1.26	–	30	[37]
PSF/N-PMMA DLHF	PSF/PVP	PSF/N-PMMA/PVP	Dry-wet spinning method	3.95	60.8	–	[38]
MMM (M6)	PES/PVP	PES/PVP/AC	Dry-wet spinning method	2.61	–	30	[41]
MMM-OIF	PES/PVP	PES/PVP/AC	Dry-wet via immersion precipitate	76.92	–	62	[40]

Table 5 Antibacterial rate of DLHF membranes against *E. coli* and *S. aureus* with initial concentration of 10^8 CFU/mL.

Membranes	Antibacterial rate (%)	
	E. coli	*S. aureus*
M0	50 ± 3.0	50 ± 2.0
M01	67 ± 2.0	62.5 ± 2.4
M02	68 ± 2.6	75 ± 2.0

3.4. Biocompatibility analysis

Percentage of NO and H_2O_2 scavenging activities of the DLHF membrane can be observed in Fig. 10. As shown in Fig. 10, M02 membrane exhibited better antioxidant defence against NO. Meanwhile, the DLHF membrane without the incorporation of silica/α-mangostin nanoparticle in the inner layer, M01 showed lower percentage of scavenging activities. Presence of the silica/α-mangostin nanoparticle in the inner layer of the DLHF membrane inhibited the nitrite formation. The hydroxyl group in the nanoparticle binds to the NO radical and formed a transition state of H-O bond, prevented the binding of the oxygen with the oxides of nitrogen, thus reduced the nitrite ions production [44,45].

Fig. 11 shows the percentage of H_2O_2 scavenging activity of the DLHF membrane. Based on Fig. 11, M02 membrane had the highest percentage of H_2O_2 scavenging activity compared to M01 and M0. Functional hydroxyl groups in silica/α-mangostin nanoparticle quenched free radicals by donating its electron and provide antioxidant effect to the body, thus preventing ROS formation. In haemodialysis patient, H_2O_2 free radicals are produced due to the reduction in antioxidant concentration and rapidly increases oxidative stress in patient. Biocompatible adsorbent in the inner layer which near the blood/membrane interface helps in scavenging these free radicals and preventing biological injury.

C5a complement activation of DLHF membrane can be observed in Fig. 12. 67.69 ng/mL of C5a was expressed when

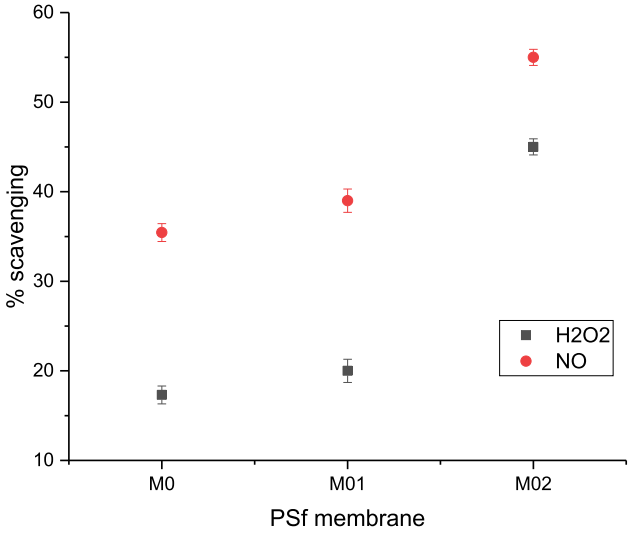

Fig. 11 Percentage of NO and H_2O_2 scavenging activities for DLHF membranes. Standard deviation is represented by the error bars (n = 3).

the plasma was immersed in control sample. The C5a concentration was reduced to 59.23 ng/mL after the introduction of the plasma with M0. The reduction of C5a expression was due to the presence of PVP in the membrane that was responsible in the reduction of the hydrophobic nature of PSf. M01 showed no significant changes compared to neat, M0 membrane, as the composition of the inner layer of M01 was the same as the neat membrane. The presence of AC in the outer layer of the membrane did not give effect to the membrane, as there was no direct contact between the plasma and AC. Meanwhile, M02 membrane showed a reduction of C5a expression of 49.23 ng/mL. Free hydroxyl group presented in the silica/α-mangostin nanoparticle inhibited the C5a expression by preventing vitamin K from working properly in coagulation cascade, thus improved the membrane biocompatibility.

Based on the sieving curves shown in Fig. 13, all the membranes allowed the small molecules uremic toxins like urea and

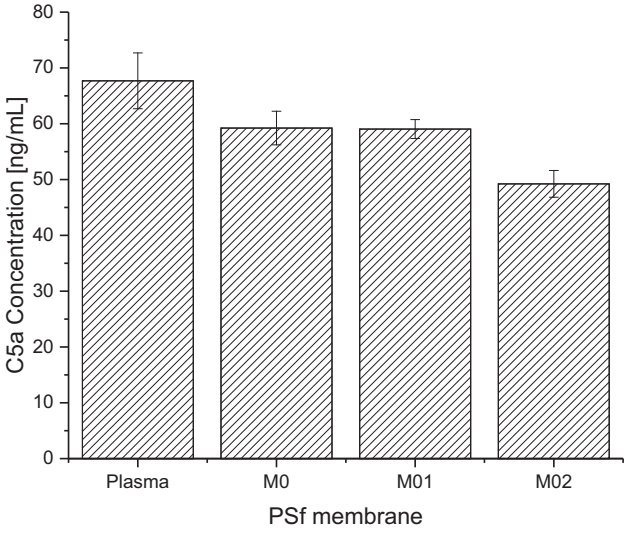

Fig. 12 C5a expression of the DLHF membranes. Standard deviation is represented by the error bars ($n = 3$).

creatine with molecular weight of 60 and 112 Da, respectively to pass through the membrane easily. In the meantime, larger size BSA was unable to pass through the membrane. For an efficient haemodialysis membrane, the membrane must be able to allow filtration of uremic toxins while prevent the transport of protein out from the membrane. From this result, it was indicated that DLHF membrane with different adsorbents in inner and outer layer of the membrane possessed excellent selectivity for haemodialysis. (SC = 1 indicates total penetration of solute, SC = 0 indicates no penetration of solute through the membrane).

4. Conclusion

DLHF membranes with different combinations of inner and outer layer compositions were successfully fabricated via a single-step co-extrusion technique. The membranes provide significant benefits to both separation performance and bacteria removal. DLHF membrane with silica/α-mangostin and AC in the inner and outer layer of the membrane, respectively showed better results as compared to SLHF membrane. The permeability of the DLHF membranes added with AC in the outer layer was improved by 54.5%. Furthermore, AC had been proven to enhance the inhibition of bacteria by preventing the bacteria from passing through the membrane, thus produced membrane with excellent antibacterial property. DLHF membrane with the combination of silica/α-mangostin nanoparticle in the inner layer, and AC in the outer layer, showed the highest percentage of urea and creatinine removal of 60.6% and 75.2%, respectively. In addition, the employment of biocompatible organic–inorganic nanofiller in haemodialysis membrane could progressively diversify its potential in this biomedical-device application. The ingenious approach which combined both unique properties of inorganic nanoparticle and versatility of polymer as a host showed great potential to combat the biocompatibility issues commonly faced by polymeric membranes.

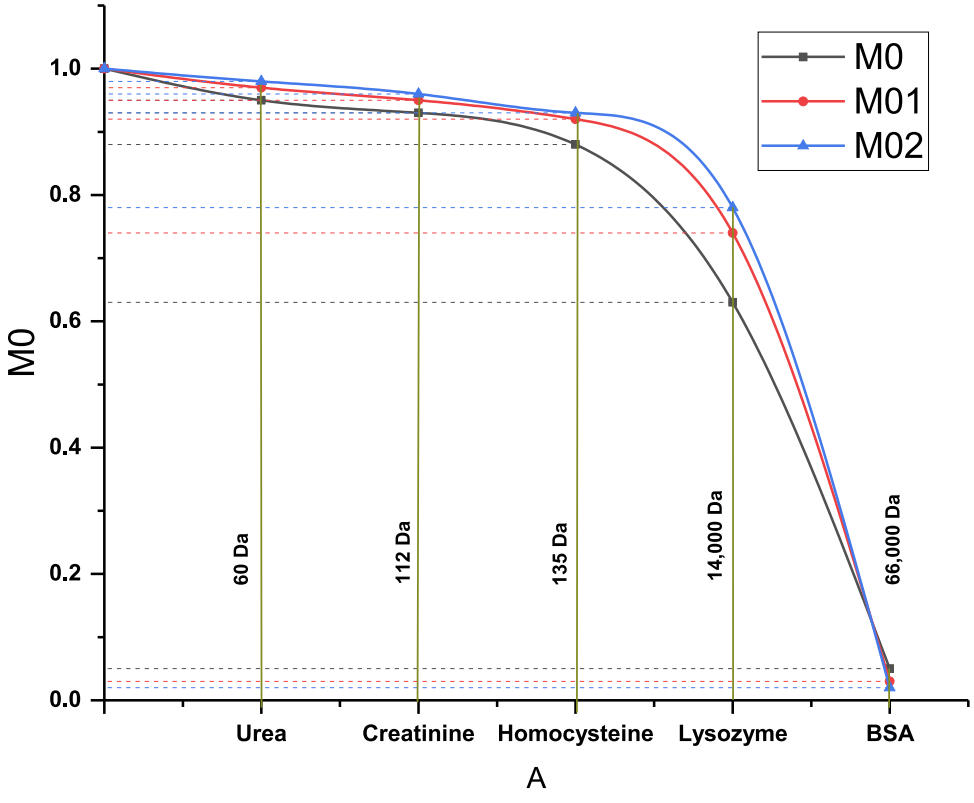

Fig. 13 Sieving curve of DLHF membrane based on several molecular weight marker.

Declaration of Competing Interest

The authors declare that they have no known competing financial interests or personal relationships that could have appeared to influence the work reported in this paper.

Acknowledgement

The authors acknowledge the financial support from Ministry of Higher Education Malaysia for the Prototype Research Grant Scheme (Project number: R.J130000.7809.4L704), and Universiti Teknologi Malaysia (UTM) under Flagship Program (Project number: Q.J130000.2409.01G46) and Industry-International Incentive Grant (Project number: Q.J130000.3609.03M17). Finally, the authors grateful to Research Management Centre, UTM for the support provided.

References

[1] O.F. Kohn, M. Plascencia, Y. Taylor, J.L. Koyner, Novel use of premixed dialysate bags during water supply interruption in acute hospital setting, Kidney360 2 (2021) 339–343, https://doi.org/10.34067/kid.0004762020.

[2] W.K. Yiek, O. Coenen, M. Nillesen, J. van Ingen, E. Bowles, A. Tostmann, Outbreaks of healthcare-associated infections linked to water-containing hospital equipment: a literature review, Antimicrob. Resist. Infect. Control. 10 (2021) 1–19, https://doi.org/10.1186/s13756-021-00935-6.

[3] H. Minasyan, Sepsis: mechanisms of bacterial injury to the patient, Scand. J. Trauma. Resusc. Emerg. Med. 27 (2019) 1–22, https://doi.org/10.1186/s13049-019-0596-4.

[4] A.D. Coulliette, M.J. Arduino, Hemodialysis and water quality, Semin. Dial. 26 (2013) 427–438, https://doi.org/10.1111/sdi.12113.

[5] A. Dewitte, S. Lepreux, J. Villeneuve, C. Rigothier, C. Combe, A. Ouattara, J. Ripoche, Blood platelets and sepsis pathophysiology: a new therapeutic prospect in critical ill patients?, Ann Intensive Care. 7 (2017), https://doi.org/10.1186/s13613-017-0337-7.

[6] K.N. Ekdahl, J.D. Lambris, H. Elwing, D. Ricklin, P.H. Nilsson, Y. Teramura, I.A. Nicholls, B. Nilsson, Innate immunity activation on biomaterial surfaces: a mechanistic model and coping strategies, Adv. Drug Deliv. Rev. 63 (2011) 1042–1050, https://doi.org/10.1016/j.addr.2011.06.012.

[7] S. Kany, J.T. Vollrath, B. Relja, Cytokines in inflammatory disease 炎症性疾患におけるサイトカイン, Int. J. Mol. Sci. 20 (2019) 1–31.

[8] O. Azhar, Z. Jahan, F. Sher, M.B.K. Niazi, S.J. Kakar, M. Shahid, Cellulose acetate-polyvinyl alcohol blend hemodialysis membranes integrated with dialysis performance and high biocompatibility, Mater. Sci. Eng. C. 126 (2021) 112127, https://doi.org/10.1016/j.msec.2021.112127.

[9] H. Waheed, S. Farrukh, A. Hussain, A. Mukhtar, M. Mubashir, S. Saqib, S. Ullah, A.P. Peter, K.S. Khoo, P.L. Show, Green synthesized nano-cellulose polyethylene imine-based biological membrane, Food Chem. Toxicol. 160 (2022) 112773, https://doi.org/10.1016/j.fct.2021.112773.

[10] E. Salimi, A. Ghaee, A.F. Ismail, M. Hafi, G.P. Sean, Current Approaches in Improving Hemocompatibility of Polymeric Membranes for Biomedical Application, (n.d.) 771–800.

[11] N. Said, W.J. Lau, Y.C. Ho, S.K. Lim, M.N. Zainol Abidin, A. F. Ismail, A review of commercial developments and recent laboratory research of dialyzers and membranes for hemodialysis application, Membr. (Basel) 11 (2021) 1–38, https://doi.org/10.3390/membranes11100767.

[12] P. Ciceri, M. Cozzolino, Expanded haemodialysis as a current strategy to remove uremic toxins, Toxins (Basel). 13 (2021) 1–14, https://doi.org/10.3390/toxins13060380.

[13] U. Eduok, A. Abdelrasoul, A. Shoker, H. Doan, Recent developments, current challenges and future perspectives on cellulosic hemodialysis membranes for highly efficient clearance of uremic toxins, Mater. Today Commun. 27 (2021) 102183, https://doi.org/10.1016/j.mtcomm.2021.102183.

[14] C.A. Falconi, C.V. da C. Junho, F. Fogaça-Ruiz, I.C.S. Vernier, R.S. da Cunha, A.E.M. Stinghen, M.S. Carneiro-Ramos, Uremic toxins: an alarming danger concerning the cardiovascular system, Front. Physiol. 12 (2021) 1–20, https://doi.org/10.3389/fphys.2021.686249.

[15] T. Banerjee, T.W. Meyer, T. Shafi, T.H. Hostetter, M. Melamed, Y. Zhu, N.R. Powe, Free and total p-cresol sulfate levels and infectious hospitalizations in hemodialysis patients in CHOICE and HEMO, Med. (United States). 96 (2017), https://doi.org/10.1097/MD.0000000000005799.

[16] C.J. Lin, H.H. Chen, C.F. Pan, C.K. Chuang, T.J. Wang, F.J. Sun, C.J. Wu, P-cresylsulfate and indoxyl sulfate level at different stages of chronic kidney disease, J. Clin. Lab. Anal. 25 (2011) 191–197, https://doi.org/10.1002/jcla.20456.

[17] B.K. Meijers, V. Weber, B. Bammens, W. Dehaen, K. Verbeke, D. Falkenhagen, P. Evenepoel, Removal of the uremic retention solute p-cresol using fractionated plasma separation and adsorption, Artif. Organs. 32 (2008) 214–219, https://doi.org/10.1111/j.1525-1594.2007.00525.x.

[18] G.A. Kaysen, The microinflammatory state in uremia: causes and potential consequences, J. Am. Soc. Nephrol. 12 (2001) 1549–1557.

[19] F. Galli, Protein damage and inflammation in uraemia and dialysis patients, Nephrol. Dial. Transplant. 22 (2007) 20–36, https://doi.org/10.1093/ndt/gfm294.

[20] K. Sakurai, Biomarkers for evaluation of clinical outcomes of hemodiafiltration, Blood Purif. 35 (2013) 64–68, https://doi.org/10.1159/000346364.

[21] R. Raoufinia, A. Mota, N. Keyhanvar, F. Safari, S. Shamekhi, J. Abdolalizadeh, Overview of albumin and its purification methods, Adv. Pharm. Bull. 6 (2016) 495–507. https://doi.org/10.15171/apb.2016.063.

[22] M. Henrie, C. Ford, M. Andersen, E. Stroup, J. Diaz-Buxo, B. Madsen, D. Britt, C.H. Ho, In vitro assessment of dialysis membrane as an endotoxin transfer barrier: Geometry, morphology, and permeability, Artif. Organs. 32 (2008) 701–710, https://doi.org/10.1111/j.1525-1594.2008.00592.x.

[23] I. Geremia, J.A.W. Jong, C.F. van Nostrum, W.E. Hennink, K. G.F. Gerritsen, D. Stamatialis, New mixed matrix membrane for the removal of urea from dialysate solution, Sep. Purif. Technol. 277 (2021) 119408, https://doi.org/10.1016/j.seppur.2021.119408.

[24] M.K. van Gelder, J.A.W. Jong, L. Folkertsma, Y. Guo, C. Blüchel, M.C. Verhaar, M. Odijk, C.F. Van Nostrum, W.E. Hennink, K.G.F. Gerritsen, Urea removal strategies for dialysate regeneration in a wearable artificial kidney, Biomaterials 234 (2020) 119735, https://doi.org/10.1016/j.biomaterials.2019.119735.

[25] M. Nidzhom, Z. Abidin, P.S. Goh, A.F. Ismail, N. Said, Highly adsorptive oxidized starch nanoparticles for efficient urea removal 201 (2018) 257–263. <https://doi.org/10.1016/j.carbpol.2018.08.069>.

[26] I. Geremia, R. Bansal, D. Stamatialis, In vitro assessment of mixed matrix hemodialysis membrane for achieving endotoxin-free dialysate combined with high removal of uremic toxins from human plasma, Acta Biomater. 90 (2019) 100–111, https://doi.org/10.1016/j.actbio.2019.04.009.

[27] M.Z. Fahmi, M. Wathoniyyah, M. Khasanah, Y. Rahardjo, S. Wafiroh, Abdulloh Incorporation of graphene oxide in polyethersulfone mixed matrix membranes to enhance hemodialysis membrane performance, RSC Adv. 8 (2018) 931–937, https://doi.org/10.1039/c7ra11247e.

[28] M.S.L. Tijink, M. Wester, J. Sun, A. Saris, L.A.M. Bolhuis-Versteeg, S. Saiful, J.A. Joles, Z. Borneman, M. Wessling, D.F. Stamatialis, A novel approach for blood purification: mixed-matrix membranes combining diffusion and adsorption in one step, Acta Biomater. 8 (2012) 2279–2287, https://doi.org/10.1016/j.actbio.2012.03.008.

[29] S. Mansur, M.H.D. Othman, M.N.Z. Abidin, A.F. Ismail, S.H. S. Abdul Kadir, P.S. Goh, H. Hasbullah, B.C. Ng, M.S. Abdullah, R. Mustafar, Enhanced adsorption and biocompatibility of polysulfone hollow fibre membrane via the addition of silica/alpha-mangostin hybrid nanoparticle for uremic toxins removal, J. Environ Chem. Eng. 9 (2021) 106141, https://doi.org/10.1016/j.jece.2021.106141.

[30] H. Dzinun, M. Hafiz, D. Othman, A. Fauzi, M. Hafiz, M.A. Rahman, J. Jaafar, Photocatalytic degradation of nonylphenol by immobilized TiO 2 in dual layer hollow fibre membranes, Chem. Eng. J. 269 (2015) 255–261, https://doi.org/10.1016/j.cej.2015.01.114.

[31] M.N.Z. Abidin, P.S. Goh, N. Said, A.F. Ismail, M.H.D. Othman, M.S. Abdullah, B.C. Ng, H. Hasbullah, S.H. Sheikh Abdul Kadir, F. Kamal, S. Mansur, Polysulfone/amino-silanized poly(methyl methacrylate) dual layer hollow fiber membrane for uremic toxin separation, Sep. Purif. Technol. 236 (2020). < https://doi.org/10.1016/j.seppur.2019.116216 > .

[32] T. Nguyen, F.A. Roddick, L. Fan, Biofouling of water treatment membranes: a review of the underlying causes, monitoring techniques and control measures, Membranes (Basel). 2 (2012) 804–840, https://doi.org/10.3390/membranes2040804.

[33] K. Rambabu, G. Bharath, P. Monash, S. Velu, F. Banat, M. Naushad, G. Arthanareeswaran, P. Loke Show, Effective treatment of dye polluted wastewater using nanoporous CaCl2 modified polyethersulfone membrane, Process Saf. Environ. Prot. 124 (2019) 266–278, https://doi.org/10.1016/j.psep.2019.02.015.

[34] S. Zheng, M. Bawazir, A. Dhall, H.E. Kim, L. He, J. Heo, G. Hwang, Implication of surface properties, bacterial motility, and hydrodynamic conditions on bacterial surface sensing and their initial adhesion, Front. Bioeng. Biotechnol. 9 (2021) 1–22, https://doi.org/10.3389/fbioe.2021.643722.

[35] D. Ngo, H. Liu, Z. Chen, H. Kaya, T.J. Zimudzi, S. Gin, T. Mahadevan, J. Du, S.H. Kim, Hydrogen bonding interactions of H2O and SiOH on a boroaluminosilicate glass corroded in aqueous solution, Npj Mater. Degrad. 4 (2020) 1–14, https://doi.org/10.1038/s41529-019-0105-2.

[36] I. Geremia, D. Pavlenko, K. Maksymow, M. Rüth, H.D. Lemke, D. Stamatialis, Ex vivo evaluation of the blood compatibility of mixed matrix haemodialysis membranes, Acta Biomater. 111 (2020) 118–128, https://doi.org/10.1016/j.actbio.2020.05.016.

[37] D. Pavlenko, E. Van Geffen, M.J. Van Steenbergen, G. Glorieux, New low-flux mixed matrix membranes that offer superior removal of protein-bound toxins from human plasma, Nat. Publ. Gr. (2016) 1–9, https://doi.org/10.1038/srep34429.

[38] M.N.Z. Abidin, P.S. Goh, N. Said, A.F. Ismail, M.H.D. Othman, M.S. Abdullah, B.C. Ng, H. Hasbullah, S.H. Sheikh Abdul Kadir, F. Kamal, S. Mansur, Polysulfone/amino-silanized poly(methyl methacrylate) dual layer hollow fiber membrane for uremic toxin separation, Sep. Purif. Technol. (2019). < https://doi.org/10.1016/j.seppur.2019.116216 > .

[39] Z. Saiful, M. Borneman, Wessling, Double layer mixed matrix membrane adsorbers improving capacity and safety hemodialysis, IOP Conf. Ser. Mater. Sci. Eng. 352 (2018) 3–9, https://doi.org/10.1088/1757-899X/352/1/012048.

[40] O.E.M. ter Beek, M.K. van Gelder, C. Lokhorst, D.H.M. Hazenbrink, B.H. Lentferink, K.G.F. Gerritsen, D. Stamatialis, In vitro study of dual layer mixed matrix hollow fiber membranes for outside-in filtration of human blood plasma, Acta Biomater. (2021), https://doi.org/10.1016/j.actbio.2020.12.063.

[41] D. Pavlenko, D. Giasafaki, G. Charalambopoulou, E. Van Geffen, K.G.F. Gerritsen, T. Steriotis, D. Stamatialis, Carbon adsorbents with dual porosity for efficient removal of uremic toxins and cytokines from human plasma, Sci. Rep. 7 (2017) 1–7, https://doi.org/10.1038/s41598-017-15116-y.

[42] A. Hashimoto-gotoh, T. Matsuki, T. Miyazawa, Evaluation of membrane filtration system using The " Pore Diffusion " for eliminating viruses, 2015. < https://doi.org/10.1292/jvms.14-0625 > .

[43] J.K. Brennan, K.T. Thomson, K.E. Gubbins, Adsorption of Water in Activated Carbons : Effects of Pore Blocking and Connectivity (2002) 5438–5447.

[44] F. Boora, E. Chirisa, S. Mukanganyama, Evaluation of nitrite radical scavenging properties of selected zimbabwean plant extracts and their phytoconstituents, J. Food Process. 2014 (2014) 1–7, https://doi.org/10.1155/2014/918018.

[45] A. Martínez, A. Galano, R. Vargas, Free radical scavenger properties of α-mangostin: thermodynamics and kinetics of HAT and RAF mechanisms, J. Phys. Chem. B. 115 (2011) 12591–12598, https://doi.org/10.1021/jp205496u.